Electrical and Photosensitive Characteristics of a-IGZO TFTs Related to Oxygen Vacancy

Jianke Yao, Ningsheng Xu, Shaozhi Deng, Jun Chen, Juncong She,
Han-Ping David Shieh, *Fellow, IEEE*, Po-Tsun Liu, *Senior Member, IEEE*, and Yi-Pai Huang

***Abstract*—The electrical and photosensitive characteristics of amorphous indium–gallium–zinc-oxide (a-IGZO) thin-film transistors (TFTs) related to the oxygen vacancies $\ddot{V}_O$ are discussed. With the filling of $\ddot{V}_O$ of ratio from 14 to 8, the electron density of the a-IGZO channel decreases from 7.5 to 3.8 ($\times 10^{16}$ cm^{-3}); the saturation mobility of the TFT decreases from 3.1 to 1.4 cm^2/(V $\cdot$ s); the threshold voltage increases from 7 to 11 V for the TFT with a lower on-current; and the subthreshold slope increases from 2.4 to 4.4 V/dec for the TFT with a higher interface defect density of 4.9 $\times$ 10^{11} cm^{-2}, the worst electrical stability of $\Delta V_{\mathrm{th}} \sim 10$ V, and a hysteresis-voltage decrease from 3.5 to 2 V. The photoreaction properties of a-IGZO TFTs are also sensitive to the oxygen-content-related absorption of the a-IGZO channel. With the lowest content of oxygen in the channel, the TFT has the largest photocurrent gain of 50 μA ($V_g = 30$ V; $V_d = 10$ V) and decrease in V_{th} ($|\Delta V_{\mathrm{th}}| \sim 5$ V) at a high light intensity. The light-induced change of TFT characteristics is totally reversible with the time constant for recovery of about 2.5 h.**

***Index Terms*—Absorption, amorphous indium–gallium–zinc–oxide (a-IGZO) thin-film transistor (TFT), electrical and photosensitive characteristics, oxygen vacancies.**

I. Introduction

THE AMORPHOUS $InGaZnO_4$ (a-IGZO) thin-film transistor (TFT), due to its superior characteristics such as high field-effect mobility, low threshold voltage, transparent and low-temperature deposition, etc., is now studied for large-area devices such as TFT backplanes in flat-panel displays [1]. As the n-type oxide semiconductor, a well-known mechanism in a-IGZO for doping is that the oxygen vacancy $\ddot{V}_O$ generates two free electrons in the conductor band and works as a shallow donor. The electron concentration changes with the O content in the a-IGZO film, which influences the electrical characteristic of the a-IGZO TFT greatly [2]. For display application, aside from the stability under the bias/current stress, the light sensitivity of the a-IGZO TFT, particularly the influence of irradiation with visible light is of great importance [3]. Due to the amorphous structure, a significant contribution of defect states to the absorption is expected. It is also known that the absorption depends on the electron concentration of the film [4]. Therefore, it is useful to know how the O content in the a-IGZO channel affects the light sensitivity of the a-IGZO TFT.

Despite the great progress in the device development [5], [6], there is a little report of the relation between the channel composition and the TFT performance, e.g., how $\ddot{V}_O$ affects the reliability for optimizing the deposition process of the TFT, because the developing of other high-stability materials such as ZrInZnO [7] or HfInZnO [8] TFTs will not only increase the manufacture cost but also lose the virtues of a-IGZO. Furthermore, the mechanisms of the enhanced reliability are seldom studied. About the photosensitivity of the a-IGZO TFT, mainly the effects of the passivation layer [9], the device structure [10], and the photostability [11] are studied, and the effect of the $\ddot{V}_O$ value of a-IGZO is seldom researched for controlling its optical properties and reducing the deposition process of the TFT. The recover dynamics of the TFT after photo illumination are rarely discussed either, which is very important for application in the display panel.

In this paper, the relation between the content of the $\ddot{V}_O$ value of the a-IGZO channel and the electrical and photosensitive characteristics of the a-IGZO TFT is discussed. In particular, the mechanism of the electrical-stress reliability and the photo responsibility of the TFT affected by $\ddot{V}_O$ are discussed. The recover dynamics of the TFT after photo illumination are also discussed.

II. Experiment

The TFTs of the bottom-gate structure are fabricated on the substrates of the n-type silicon wafer using the shadow-mask process. The substrates are cleaned by acetone, methanol, and deionized water in an ultrasonic bath in turn. A 100-nm-thick SiO_2 layer is thermally oxidized on the substrate in a furnace (> 1100 °C). As the active layer, 40-nm a-IGZO thin films are deposited by radio-frequency (RF) magnetron sputter using a $InGaZnO_7$ target at room temperature with a flow rate of 10 sccm for the Ar gas and different flow rates of the O_2 gas (from 0 to 2 sccm) for controlling the oxygen content in the film, and the sputtering power is 80 W. Then, the source/drain electrodes of the 40-nm-thick indium tin oxide are deposited by RF magnetron sputter. The TFT channel is designed with a width of $W = 2$ mm and a length of $L = 100$ μm. After fabrication, the TFTs are annealed in a N_2 atmosphere at 350 °C for 1 h to improve the electrical property and reliability.

Manuscript received September 21, 2010; revised December 14, 2010 and December 31, 2010; accepted January 5, 2011. Date of publication March 14, 2011; date of current version March 23, 2011. The review of this paper was arranged by Editor H.-S. Tae.

J. Yao, N. Xu, S. Deng, J. Chen, and J. She are with the State Key Laboratory of Optoelectronic Materials and Technologies, Guangdong Province Key Laboratory of Display Materials and Technologies, Sun Yat-Sen University, Guangzhou 510275, China.

H.-P. D. Shieh, P.-T. Liu, and Y.-P. Huang are with the Department of Photonics and the Display Institute, National Chiao Tung University, Hsinchu 300, Taiwan (e-mail: hpshieh@mail.nctu.edu.tw).

Color versions of one or more of the figures in this paper are available online at http://ieeexplore.ieee.org.

Digital Object Identifier 10.1109/TED.2011.2105879

0018-9383/$26.00 © 2011 IEEE

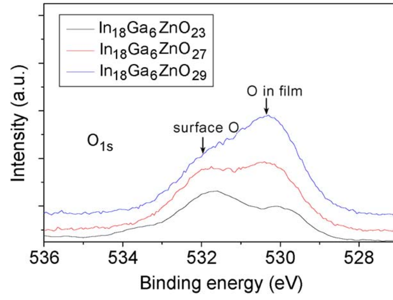

Fig. 1. XPS spectra of a-IGZO films.

The oxygen content of a-IGZO films are measured by X-ray photoemission spectroscopy (XPS; Thermo VG ESCALab 250). The absorption spectra of a-IGZO films are measured with a Lambda 900 spectrometer. The sheet resistivity R of a-IGZO films are measured by the four-probe method. The electrical properties of the TFT are tested by a semiconductor parameter analyzer (Keithley SCS 4200). The measurements of electrical properties for films and TFTs are made on at least three film samples and six devices with different oxygen contents. While studying the photoreaction, the TFTs are exposed to the light of a light-emitting diode with $\lambda = 425$ nm and the power density P_d increased from 1 to 10 mW/cm^2. A sequence of electrical characteristics are recorded and studied with the increasing P_d. All calculation equations for the TFT are referred from Kagan and Andry [12].

III. Electrical Characteristics

Fig. 1 shows the XPS spectra of O_{1s} in a-IGZO films. The peaks are clearly resolved into two components centered at 530 and 532 eV. The low-binding-energy component centered at 530 eV is attributed to O^{2-} ions in a-IGZO. The high-binding-energy peak located at 532 eV is corresponding to the existence of weakly bound oxygen species on the films' surface such as $-CO_3$, $-OH$, or adsorbed O_2 [13]. It is found that the peak area of O in the film increases while that of the surface O is almost constant for the three a-IGZO films. The peak energies of the surface oxygen and the oxygen in the film for three films are almost the same, respectively. The calculated atom ratio from the peak area is listed in Fig. 1. It is found that all the atom ratios of ZnO, Ga_2O_3, and In_2O_3 are the same, i.e.,1:3:9 (calculated by XPS results), while those of the deficient oxygen decrease from 14 to 10 to 8, indicating the filling of $\ddot{V}_O$ and the decrease in the electron concentration, as inferred from the defect equation of a-IGZO, i.e.,

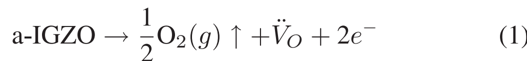

$$\text{a-IGZO} \rightarrow \frac{1}{2}O_2(g) \uparrow + \ddot{V}_O + 2e^- \tag{1}$$

with the rule that stoichiometric a-InGaZnO$_4$ is intrinsic because the sum of charges is zero.

The measured sheet resistivity R and the calculated electrical conductivity σ by equation $\sigma = 1/(Rd)$ for a-IGZO films are listed in Table I, in which d is the thickness of the film. It is found that R increases and σ decreases with the increase in the O content in the a-IGZO film due to the film being closer to stoichiometric with fewer structural defects. Fig. 2 shows the transfer characteristics of a-IGZO TFTs with parameters summarized in Table I. All data in Table I are showed with mean values and standard deviation. It is found that the oxygen content of the a-IGZO channel has significant effects on the device performance. With the increase in the oxygen content, the on-current I_{on} and the saturation mobility μ_s decrease, and the threshold voltage V_{th} and the subthreshold slope S increase. The electron density N_e in the a-IGZO channel corresponding to the turn-on voltage V_{on} is estimated as

TABLE I
Summary of TFT Performance Parameters

Parameters \ Channel	$In_{18}Ga_6ZnO_{23}$	$In_{18}Ga_6ZnO_{27}$	$In_{18}Ga_6ZnO_{29}$
R (KΩ/□)	2.5±0.2	3.2±0.1	7.1±0.1
σ (10^2S/cm)	1.0±0.1	0.8±0.1	0.4±0.1
μ_s(cm^2/(V.s))	3.1±0.4	2.0±0.2	1.4±0.3
V_{th} (V)	7±2	8±1	11±2
S (V/dec)	2.4±0.2	2.8±0.1	4.4±0.2
N_i (10^{11} cm^{-2})	2.3±0.3	2.8±0.1	4.9±0.3
ΔV_{th} (V)	4.5±0.2	5±0.1	10±0.3
V_{on} (V)	-4±1	-3±1	-2±1
N_e (10^{16}cm^{-3})	7.5±0.3	5.6±0.1	3.8±0.3
ΔV_h (V)	3.5±0.4	2.5±0.2	2±0.4

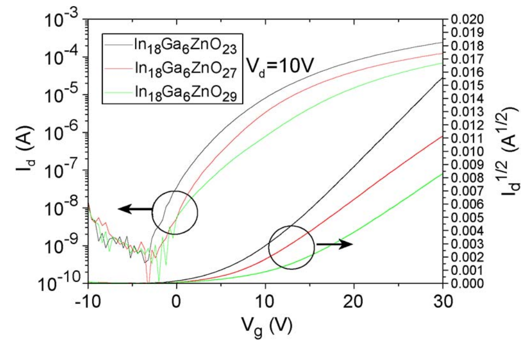

Fig. 2. Transfer characteristics of a-IGZO TFTs.

$$N_e = \frac{C_i V_{\text{on}}}{q t_c} \tag{2}$$

where C_i is the gate insulator capacitance per unit area, q is the elementary charge, and t_c is the thickness of the channel layer. In this case, $C_i = 12$ nF/cm^2, and $t_c = 40$ nm. As shown in Table I, N_e decreases with the increasing O content, and this is consistent with the XPS results. As for the n-type TFT, V_{th} decreases, and μ_s increases for the high-N_e channel, leading to high I_{on}, as referred from the equation of the drain current in the saturation region $(V_d > V_g - V_{\text{th}})$, i.e.,

$$I_d = \frac{C_i \mu_s W}{2L}(V_g - V_{\text{th}})^2. \tag{3}$$

The interface-state defect densities N_i are calculated by

$$N_i = \left[\frac{\lg(e)S}{kT/q} - 1\right]\frac{C_i}{q} \tag{4}$$

where e is the constant, S is the subthreshold slope, q is the electron charge, k is the Boltzmann constant, and T is the temperature.

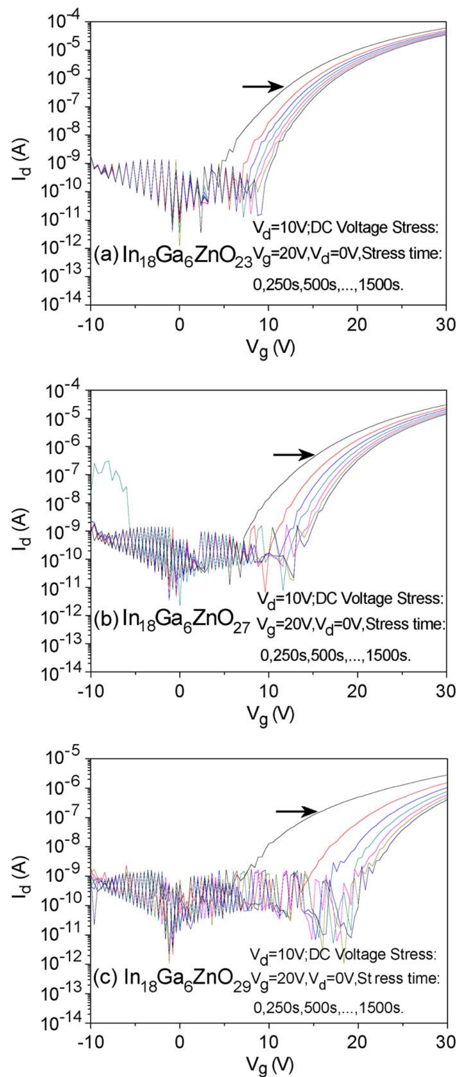

Fig. 3. Electrical-stress time evolution of the I_d–V_g characteristics for a-IGZO TFTs.

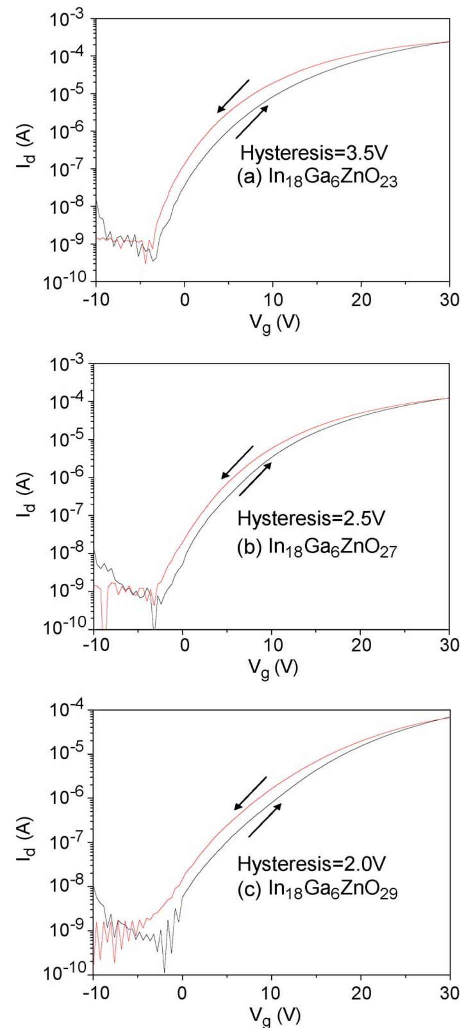

Fig. 4. Hysteresis curves for a-IGZO TFTs.

Fig. 3 shows the positive gate voltage stress (PGVS) induced shift of the transfer curve. The calculated $\Delta V_{\rm th}$ values after a 1500-s stress are listed in Table I. It can be seen that $\Delta V_{\rm th}$ increases and the stability decreases for the TFT with a higher O content in the channel, which is due to the fact that the TFT has higher $V_{\rm th}$. Generally, the TFT with higher $V_{\rm th}$ has more defects at the interface between the channel and the dielectric, as seen from the calculated N_i, and has worse stability, as discussed in [14], i.e., the TFT with large positive $V_{\rm th}$ values corresponds to the TFT that is strongly influenced by the trapping in interface states and/or bulk traps in the semiconductor band gap and therefore has worse stability. The intrinsic cause is that the TFT with more $\ddot{V}_O$ in the channel has larger N_e, as shown in Table I. An increase in N_e is consistent with a shift in the zero-gate-bias Fermi level toward the conduction band. As the zero-gate-bias Fermi level shifts toward the conduction band, a larger fraction of interface traps and/or traps within the semiconductor are filled, resulting in the reduced trapping in the gate dielectric and/or at the channel/dielectric interface N_i and a corresponding increase in the electrical stability, due to the fact that the phenomenon of a positive $\Delta V_{\rm th}$ value with an applied PGVS results from the negative charge being trapped at the insulator/active interface or getting injected into the gate dielectric.

To gain more insights into the effect of the O content in the a-IGZO channel, the hysteresis of a-IGZO TFTs were examined, as shown in Fig. 4. The transfer curves were subjected to a hysteresis loop under a sweeping V_g from -10 to 30 V with the same sweep speed. $V_{\rm th}$ shifts to a more negative voltage for the hysteresis loop during the return sweep. It is found that the hysteresis value ΔV_h decreases with increasing O content in a-IGZO. The negative $V_{\rm th}$ shift indicates that electrons were detrapped at the channel/dielectric interface or rejected from the dielectric to the channel. The suppression of the hysteresis for the a-IGZO film with the higher O content is attributed to an oxygen excess leading to the decrease in the electron density and the trap states. In this case, the hysteresis and the stability of the TFT have no apparent relation.

IV. Photosensitivity

Fig. 5 shows the absorption spectra of a-IGZO films. It is found that the absorption increases with the decrease in the O content in the film. The relationship between absorption

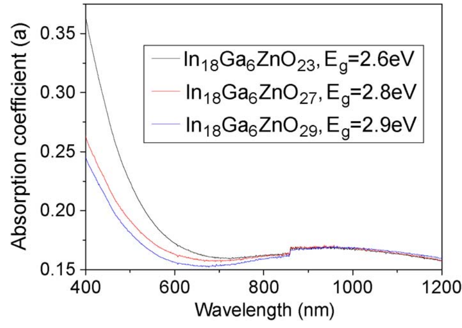

Fig. 5. Absorption spectra of a-IGZO films.

coefficient and the concentration of free electrons can be written as

$$a = \frac{N_e q^2 \lambda^2}{8\pi\varepsilon_0 n\tau m^* c^3} \tag{5}$$

where a, N_e, q, λ, ε_0, n, τ, m^*, and c are the absorption coefficient, the concentration of the free electron, the electron charge, the absorption wavelength, the dielectric constant in the vacuum, the refractive index, the relax time, the effective mass of the free electron, and the optical velocity, respectively [4]. It can be found that the absorption increases with the concentration of the free electron, which is consistent with Fig. 5. The band gap of a-IGZO films are calculated with $(\text{ahv})^{1/2} \sim (\text{hv})$ by the Tauc plot, and the values are from 2.6, 2.8, to 2.9 eV, respectively, showing the band-gap widening effect for the film with a low electron density. The result shows that only the photos with energy higher than 2.6 eV exhibited the photoelectric effect.

Fig. 6 shows the transfer characteristics of a-IGZO TFTs with an increase in the light power density P_d. While, toward higher P_d, V_{th} and, concomitantly, I_{on} show a clear saturation, a further increase in I_{off} with higher intensities can be seen. The increasing number of photo-induced carriers as P_d increases is the most plausible explanation for this trend. There are different energy levels within the semiconductor optical band gap, which is the characteristic of different defects such as deep or shallow states, in the limit; when the incident radiation has energy higher than the band gap, the photons are readily absorbed by the semiconductor. A variation of P_d is always fixed in the same energy level, changing only the number of the photo-induced charges that can be created within that energy level. Increasing P_d will allow for more energy states to be filled and will therefore allow increasing the conductivity of the channel (increasing the density of states in the volume of the semiconductor layer, thus increasing I_{off}) and facilitating the formation of the conduction channel (the charge defect states, situated near the interface between the semiconductor and the dielectric), which is the reason for lower V_{th} and higher I_{on} as P_d increases.

The extracted photocurrent gain ΔI_d, decreasing V_{th} ($|\Delta V_{\text{th}}|$), and the change of mobility μ_S are showed in Fig. 7. It can be found that ΔI_d and $|\Delta V_{\text{th}}|$ increase for the more oxygen-deficient a-IGZO channel and that μ_S values are constant during the light illumination. The photocarrier dynamics are referred from Forbes *et al.* [15]. During the photo illumination, the generation of photoelectrons ΔN can be expressed as

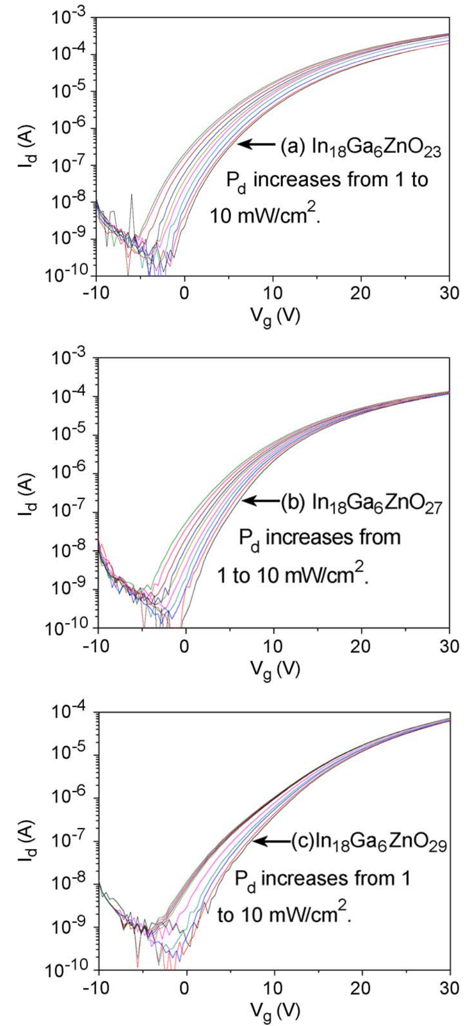

Fig. 6. Transfer characteristics of a-IGZO TFTs with an increased light power density.

$$\Delta N = \beta a I \tau_1 \left(1 - e^{-\frac{t}{\tau_1}}\right) \tag{6}$$

where β is the rate of production for photoelectrons, a is the absorption coefficient of the a-IGZO channel at $\lambda = 425$ nm as shown in Fig. 5, I is the light intensity, τ_1 is the life of photoelectrons, and t is the illumination time of 30 s in the case. ΔI_d in the saturation region can be expressed as

$$\Delta I_d = -\frac{C_i \mu_s W}{L}(V_g - V_{\text{th}})\Delta V_{\text{th}}. \tag{7}$$

Inferred from (5)–(7), with the high electron density N_e in the a-IGZO channel of the low O content, the a-IGZO channel has the highest absorption, leading the TFT with high ΔN and, therefore, large $|\Delta V_{\text{th}}|$ and ΔI_d during the photo illumination and long time to the saturation behavior, which is consistent with the results in Figs. 5–7 that the TFT with more $\ddot{V}_O$ in the channel is more sensitive to light. It can be explained that the channel has a higher density of electrons with more $\ddot{V}_O$. The absorption due to a low density of electrons can be

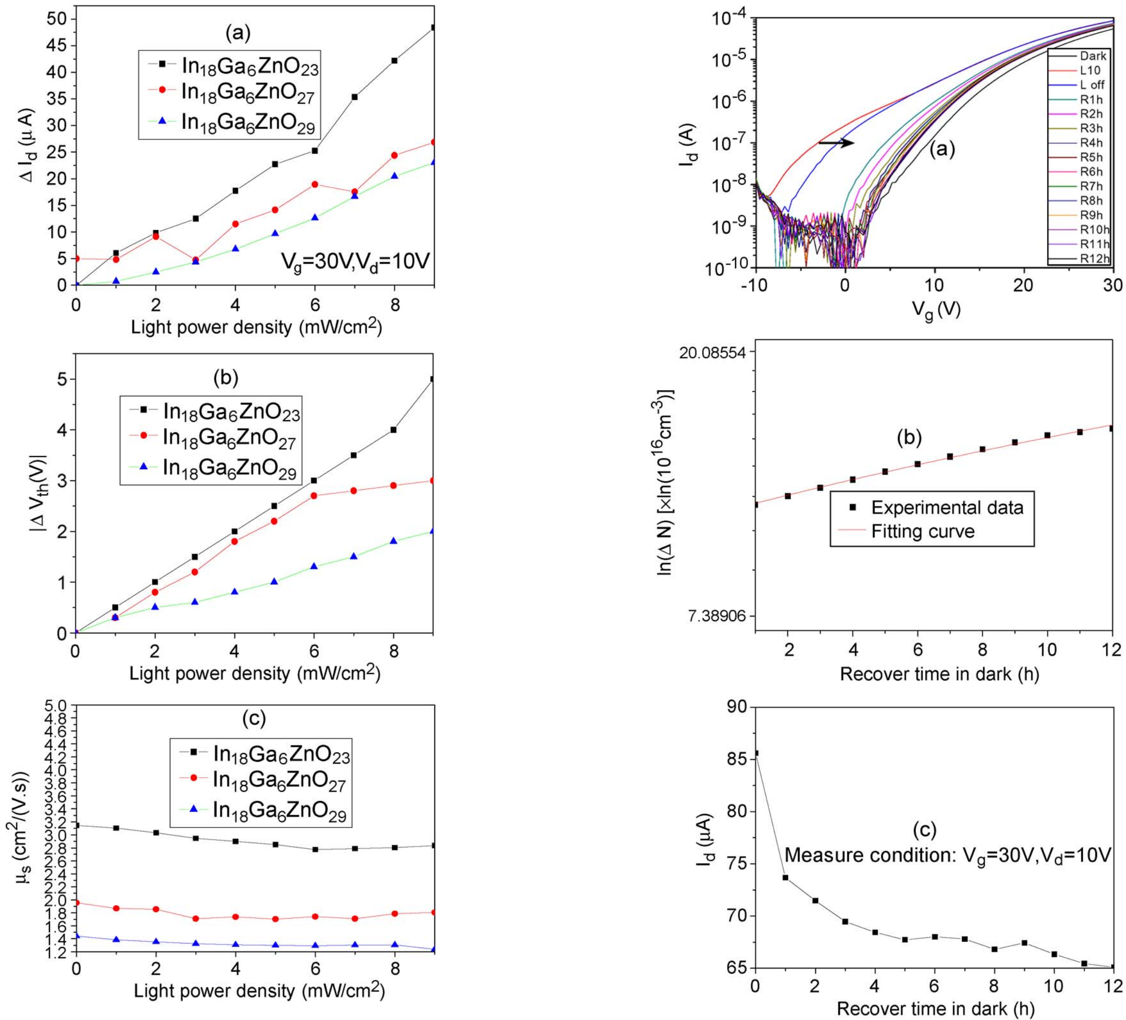

Fig. 7. Effects of light power density on the $I_{\rm on}$, $V_{\rm th}$, and μ_s values of a-IGZO TFTs.

easily bleached out at elevated light intensities (the saturable absorber). Alternatively, the occupation of a lower density of traps for charge carriers may reach its saturation value earlier (at a lower intensity and, thus, a lower charge carrier density).

The light-induced change in the TFT characteristics is totally reversible. Fig. 8 shows the recover dynamics in the dark after the photo illumination of the a-IGZO TFT with the channel of $In_{18}Ga_6ZnO_{23}$. It is found that, after the light is turned off, the transfer curve shifts to the right in 12 h to the initial dark state before the light illumination, with a decrease in I_d and an increase in $V_{\rm th}$ and μ_s. After the light is turned off, the photocarriers disappear by

$$\Delta N = \beta a I \tau_2 e^{\frac{t}{\tau_2}} \tag{8}$$

where ΔN is the decrease in the electron density N_e in the channel; t is the recovery time; τ_2 is the time constant for the recovery; and β, α, and I are the same as those in (6). N_e can be calculated by (1). ΔN as a function of the recovery time is showed in Fig. 8(b). Using relation $\ln(\Delta N) \sim t/\tau_2$, τ_2 is calculated from the slope of the fitting line. In this case, τ_2 is about 2.5 h. Different time constants for the recovery depend on the photoelectron-induced absorption, as shown in (5) and (8).

Fig. 8. Recover dynamics in the dark of the a-IGZO TFT after photo illumination with an intensity of 10 mW/cm^2. (Dark: Initial state before light illumination; L10: State after light illumination of 10 min; Loff: State of light-off; R1–R12 h: States of recover after light-off.

The photocurrent decay and the $V_{\rm th}$ recovery are shown in Fig. 8(c) and (d). Gorrn *et al.* [3] has verified that the transient of the $V_{\rm th}$ recovery and the decrease in conductivity shows a similarity. The conductivity is proportional to the density of free electrons, which can be expressed as (8). Therefore, the model [see (7) and (8)] is also valid for the photocurrent decay and the $V_{\rm th}$ recovery of the TFT, which are governed by the change of the space charge in the channel near the interface to the dielectric.

V. Conclusion

In conclusion, it has been found that the oxygen content of the a-IGZO channel has significant effects on the electrical and light-sensitivity characteristics of the a-IGZO TFT. For the a-IGZO with a higher O content of the lower density of electrons, the electrical and photosensitive characteristics of the TFT degrade. The photosensitive behavior of a-IGZO TFTs depends on the absorption of a-IGZO. For the a-IGZO channel with high absorption, the a-IGZO TFT has large photocurrent gain and shift of V_{th} after the light illumination. The light-induced change in the TFT characteristic is reversible with the recovery time constant, depending on the photoelectron-induced absorption.

References

[1] M. Ito, M. Kon, C. Miyazaki, N. Ikeda, M. Ishizaki, R. Matsubara, Y. Ugajin, and N. Sekine, "Amorphous oxide TFT and their applications in electrophoretic displays," *Phys. Stat. Sol. (A)*, vol. 205, no. 8, pp. 1885–1894, Aug. 2008.

[2] K. Nomura, H. Ohta, A. Takag, T. Kamiya, M. Hirano, and H. Hosono, "Room-temperature fabrication of transparent flexible thin-film transistors using amorphous oxide semiconductors," *Nature*, vol. 432, no. 7016, pp. 488–492, Nov. 2004.

[3] P. Görrn, M. Lehnhardt, T. Riedl, and W. Kowalsky, "The influence of visible light on transparent zinc tin oxide thin film transistors," *Appl. Phys. Lett.*, vol. 91, no. 19, pp. 193504-1–193504-3, Nov. 2007.

[4] J. K. Yao, Z. X. Fan, Y. X. Jin, Y. A. Zhao, H. B. He, and J. D. Shao, "Investigation of damage threshold to TiO_2 coatings at different laser wavelength and pulse duration," *Thin Solid Films*, vol. 516, no. 6, pp. 1237–1241, Jan. 2008.

[5] T. Kamiya, K. Nomura, and H. Hosono, "Origins of high mobility and low operation voltage of amorphous oxide TFTs: Electronic structure, electron transport, defects and doping," *J. Display Technol.*, vol. 5, no. 7, pp. 273–288, Jul. 2009.

[6] T. Kamiya, K. Nomura, and H. Hosono, "Present status of amorphous In–Ga–Zn–O thin-film transistors," *Sci. Technol. Adv. Mater.*, vol. 11, no. 4, p. 044 305, Aug. 2010.

[7] J. S. Park, K. S. Kim, Y. G. Park, Y. G. Mo, H. D. Kim, and J. K. Jeong, "Novel ZrInZnO thin-film transistor with excellent stability," *Adv. Mater.*, vol. 21, no. 3, pp. 329–333, Jan. 2009.

[8] E. Chong, K. C. Jo, and S. Y. Lee, "High stability of amorphous hafnium–indium–zinc–oxide thin film transistor," *Appl. Phys. Lett.*, vol. 96, no. 15, pp. 152102-1–152102-3, Apr. 2010.

[9] H. Zan, H. Hsueh, S. Kao, W. Chen, M. Ku, W. Tsai, and C. Tsai, "New polymer-capped a-IGZO TFT with high sensitivity to visible light for the development of integrated touch sensor array," in *Proc. SID Dig.*, 2010, pp. 1316–1318.

[10] Y. Kamada and S. Fujita, "Photo-leakage current in ZnO TFTs for transparent electronics," in *Proc. SID Dig.*, 2010, pp. 1029–1032.

[11] T. Chen, T. Chang, C. Tsai, T. Hsieh, S. Chen, C. Lin, M. Hung, C. Tu, J. Chang, and P. Chen, "Behaviors of InGaZnO thin film transistor under illuminated positive gate-bias stress," *Appl. Phys. Lett.*, vol. 97, no. 11, pp. 112104-1–112104-3, Sep. 2010.

[12] C. R. Kagan and P. Andry, *Thin Film Transistor*. New York: CRC Press, 2003.

[13] K. Remashan, D. K. Hwang, S. D. Park, J. W. Bae, G. Y. Yeom, S. J. Park, and J. H. Jang, "Effect of N_2O plasma treatment on the performance of ZnO TFTs," *Electrochem. Solid-State Lett.*, vol. 11, no. 3, pp. H55–H58, Dec. 2008.

[14] H. Q. Chiang, B. R. McFarlane, D. Hong, R. E. Presley, and J. F. Wager, "Processing effects on the stability of amorphous indium gallium zinc oxide thin-film transistors," *J. Non-Cryst. Solids*, vol. 354, no. 19–25, pp. 2826–2830, May 2008.

[15] L. Forbes, L. L. Wittmer, and K. W. Loh, "Characteristics of the indium-doped infrared sensing MOSFET (IRFET)," *IEEE Trans. Electron Devices*, vol. 23, no. 12, pp. 1272–1278, Dec. 1976.

Jianke Yao, photograph and biography not available at the time of publication.

Ningsheng Xu, photograph and biography not available at the time of publication.

Shaozhi Deng, photograph and biography not available at the time of publication.

Jun Chen, photograph and biography not available at the time of publication.

Juncong She, photograph and biography not available at the time of publication.

Han-Ping David Shieh, photograph and biography not available at the time of publication.

Po-Tsun Liu, photograph and biography not available at the time of publication.

Yi-Pai Huang, photograph and biography not available at the time of publication.